

AD-A099 204

ARIZONA UNIV TUCSON DEPT OF PHYSICS

F/G 7/4

A SURVEY OF OPTICAL CONSTANTS IN THE 5 - 25 MICRON SPECTRAL REG--ETC(U)

APR 81 D R HUFFMAN

N00019-79-C-0557

NL

UNCLASSIFIED

1 OF 1  
AD A  
009204

DTIC

END

DATE

FILMED

6-81

DTIC

AD A099204

Naval Air Systems Command  
Contract  
N00019-79-C-0557

A SURVEY OF OPTICAL CONSTANTS  
IN THE 5 - 25 MICRON SPECTRAL REGION

Final Technical Report

Principal Investigator:

Donald R. Huffman  
Department of Physics  
Univeristy of Arizona  
Tucson, Arizona 85721

March 13, 1981

DTIC  
ELECTE  
MAY 21 1981  
A

THE UNIVERSITY OF  
**ARIZONA**

81 5 21 025

APPROVED FOR PUBLIC RELEASE  
DISTRIBUTION UNLIMITED

SECURITY CLASSIFICATION OF THIS PAGE (When Data Entered)

DD FORM 1 JAN 73 1473 EDITION OF 1 NOV 65 IS OBSOLETE

UNCLASSIFIED

SECURITY CLASSIFICATION OF THIS PAGE (When Data Entered)

40-113

# ABSTRACT

A technique has been developed for determining the spectrum of optical constants in the vicinity of strong lattice absorption bands in the infrared region for solids available only in small particle form. The technique involves segregating a sub-micrometer size fraction of the sample for dispersal in infrared-transparent KBr pellets, measuring the transmission spectrum and fitting it with a combination of the Lorentz oscillator equations and small particle extinction theory, normally based on a random distribution of Rayleigh ellipsoids. The assumption that bulk optical constants apply to particles as small as 0.1  $\mu\text{m}$  is supported by careful new measurements on two small particle systems where the shapes are known to be cubes (MgO smoke) and spheres (amorphous quartz smoke). Several tests of the extinction theory for irregular shapes are discussed in cases where optical constants are well known. The method for determining optical constants has been applied to the natural silicate samples obsidian (volcanic glass), serpentine, chlorite, montmorillonite, talc, and volcanic dust from the Mt. St. Helens eruption as well as to amorphous aluminum oxide smoke. The method should be most reliable for single component, isotropic solids existing in a wide distribution of particle shapes. Particular caution is expressed in application to heterogeneous materials such as soil samples and atmospheric dust samples.

NHS GRAI	
RAC TAB	
Unannounced	<input type="checkbox"/>
Justification	<input type="checkbox"/>
Distribution/	
Availability Codes	
Avail only/or	
Part	Special
A	

## I. INTRODUCTION

When light interacts with solids and liquids the resulting effects are many and varied. Reflection from a metallic mirror surface may approach 100% and is a few per cent for glasses. Dispersion of white light on entering transparent matter at non-normal incidence provides the basis for the prism monochromator and enables nature to display its rainbow in the clouds. Wavelength dependent scattering of light by small particles provides us with the variable red hues of sunset, haloes around the sun and a very rare blueing of the moon. Wavelength dependent absorption causes the vivid red hues of the Grand Canyon as well as the dirty brown of Los Angeles smog. If our human restrictions to the visible portion of the electromagnetic spectrum were lifted, the infrared and ultraviolet regions would show even more varied sights. The basic physical parameter which underlies all these optical effects is the wavelength dependent, complex optical constant

$$m(\lambda) = n + ik$$

in which the real part is the index of refraction and  $k$  is usually called the extinction coefficient. (We will avoid this terminology in favor of simply  $k$  to prevent confusion with small particle extinction, which is the sum of absorption and scattering.)

### A. The Need for Optical Constants

Optical constants, along with suitable results from electromagnetic theory such as Snell's law, Fresnel's equations, Mie theory, etc., enable one to calculate the various

optical phenomena. From the point of view of fundamental physics the optical constants are manifestations of the energy level (or energy band) structure for the interacting atoms and molecules composing the matter, just as emission lines from gases are related to the atomic energy level structure.

Despite the importance of optical constants of solids there are no comprehensive tabulations of  $n$  and  $k$  vs wavelength for solids. This can be contrasted with the many and extensive tables of emission lines for atoms and molecules of gases.

Small particles of solid or liquid matter constituting smokes or fogs are being considered seriously by the Navy for purposes of deliberate obscuration. Because of the region of relative transparency in the atmosphere from about 8 to 14  $\mu\text{m}$  wavelength, this "10 micron region" is of particular importance. Both for the purpose of blocking  $\text{CO}_2$  laser radiation near 9.6 and 10.6  $\mu\text{m}$  and for obscuration against thermal imaging in the atmospheric window, aerosols with strong absorption bands in the 10  $\mu\text{m}$  region may be useful. Many of the natural silicate minerals which abound in the earth's crust have such strong absorption bands. However, the effort to adapt such solids for the Navy's purposes is greatly hampered by lack of the basic optical information, i.e. optical constants, for these materials.

#### B. Optical Constants of Powders

Optical constants of solids and liquids available as homogeneous bulk samples are easy to measure in spectral regions where the samples are transparent. In the highly absorbing regions of interest for infrared obscuration, the determination of optical constants is more difficult. Nevertheless, there are well known methods for determining  $n$  and  $k$  for samples of these homogeneous solids and liquids. Unfortunately, many of the most important solids which could be used as artificial aerosols for obscuration, are not available in single crystals

or otherwise homogeneous bulk form of sufficient size for the conventional optical constants determination methods to be used. They can only be obtained or synthesized as powders. Techniques for determining optical constants of powdered materials would allow a much more expanded collection of optical constants to be assembled. Unfortunately the difficulties are great, and well established procedures have not been available. In this report we present further results of the development begun in our last year's N.A.S.C. contract work aimed at understanding how to derive accurate optical constants of powdered materials in the infrared wavelength region, including the 8-14  $\mu\text{m}$  window. Using procedures from this development work optical constants for several materials will be presented.

#### C. Applicability of Bulk Optical Constants to Particles

As more concerted attempts have been made in recent years to determine optical constants of small particles and aerosols, two nagging problems have arisen concerning the applicability of the "measured" optical constants to small particle solids. Both of these problems have arisen because optical constants derived from small particles and aerosols frequently do not agree with optical constants for the constituent solid or solids. One viewpoint is that the optical constants for micron- or sub-micron size particles are substantially different from optical constants for the bulk solids. That is, optical constants are highly size-dependent in the range of particle sizes important for the practical applications. This could be a serious problem, implying that even if one had a comprehensive collection of bulk optical constants it would not be particularly useful for predicting small particle optical behavior. We do not agree with this viewpoint as will be discussed shortly. The other deduction from lack of agreement between small particle optical effects and those inferred from bulk optical constants of the solid is that the small particle

effects are representative of "effective" optical constants which, while apparently different from bulk, are the result of averaging over factors such as orientation and heterogeneous composition. The "effective" optical constants, the argument goes, are therefore the most useful and important quantities to be measured. Thus there is presently a significant feeling that (1) optical constants of small particles are significantly different from bulk solids or (2) effective or average optical constants differing from the homogeneous bulk are the appropriate quantities to measure. Because of the prevalence of these ideas several careful experiments have been carried out as reported in section III.

#### D. Plan of the Presentation

Following this introduction, section II will summarize the necessary background for bulk optical constants determinations and the theory of small particle optical effects. first for spheres and then for a distribution of shapes in so far as this can be handled in the Rayleigh ellipsoid approximation. Section III, as already indicated, reports experimental work directed specifically toward the questions of applicability of bulk optical constants to small particles. In section IV a summary of experimental techniques used in determinations of optical constants, both for bulk solids and for small particle samples, is given. Some insight into uncertainties to be expected in optical constants determinations is given by comparing results from several different authors for one type of bulk solid. Section V contains the optical constants results for solids studied in this work, and the concluding section VI summarizes the most important deductions from this work.



## II. THEORETICAL BACKGROUND

### A. Definitions of Optical Constants for Bulk Matter

A plane homogeneous electromagnetic wave propagating in the x direction has an electric field given by

$$\begin{aligned} E &= E_0 \exp \left( -\frac{2\pi k z}{\lambda} \right) \exp \left( \frac{i 2\pi n z}{\lambda} - i\omega t \right) \\ &= E_0 \exp \left( \frac{2\pi N z}{\lambda} - i\omega t \right) \end{aligned} \quad (1)$$

where the complex index of refraction is

$$N = n + ik .$$

As written in the second form above the equation allows physical meaning to be assigned to  $n$  and  $k$ . The real part of  $N$  determines the wavelength in the medium  $\lambda/n$  or the phase velocity  $v = c/n$ , while the imaginary part determines the attenuation. The pair of quantities  $\underline{n}$  and  $\underline{k}$  are known as optical constants, terminology that is as widespread as it is misleading: the optical "constants" are not constant as they often depend strongly on frequency. It is not unusual for  $k$  of many common solids to range over six orders of magnitude within a relatively narrow range of frequencies.

An alternate description of the optical properties of matter can be given by the wavelength (or frequency) dependent dielectric function which relates the electrical response of matter to a time varying electric field

$$D = \epsilon E$$

where

$$\epsilon = \epsilon_1 + i\epsilon_2 .$$

The complex dielectric function  $\epsilon$  and the complex index of refraction  $N$  are not independent but are related as follows:

$$N = \sqrt{\epsilon}$$
$$\epsilon_1 = n^2 - k^2 \quad (2)$$
$$\epsilon_2 = 2nk$$

Either of the frequency dependent quantities  $N$  or  $\epsilon$  can be said to describe the optical properties of matter. In some cases one description is more appropriate, and in other cases the other description is more appropriate. For example, in describing plane wave propagation as in equation (1) the index of refraction is simpler and more intuitively obvious, while in describing the microscopic mechanisms that are responsible for optical effects in matter,  $\epsilon$  is more appropriate.

#### B. Methods for Determining Bulk Optical Constants

The most direct determination of optical constants is accomplished by measurement of transmission through a slab and reflectance from its surface. For wavelength regions in which the absorption coefficient is very high, which include nearly all the candidates for extreme obscuration, absorption is so great that bulk solids cannot be produced, sufficiently thin that any measurable light penetrates through the slab. One must necessarily resort to reflectance techniques. Since, however, both optical constants cannot be determined from one measurement, the usual procedure is to measure reflectance under two different conditions (two polarization states at non-normal incidence or two different angles) or to measure reflectance over an extended wavelength range coupled with an analysis that properly relates  $n$  and  $k$ . We now

present more details of this last technique since our small particle method is closely related.

The normal incidence reflectance  $R$  from a surface of material characterized by optical constants  $n$  and  $k$  is given by the Fresnel equation

$$R = \frac{(n-1)^2 + k^2}{(n+1)^2 + k^2} \quad (3)$$

where the external medium in this case is assumed to be air with index of refraction of 1. If the reflectance is measured at one angle (almost-normal-incidence for example) over a wide range of wavelengths, the reflectance data can be analyzed for optical constants by a suitable integration (Kramers-Kronig analysis) of a function of the reflectance extrapolated to zero and to infinity in frequency. This often-used technique is reviewed in the article by Stern (1963). The need for extrapolation to extreme frequency regions can be circumvented by fitting the reflectance data in the range of interest with a multiple oscillator model. The solid is assumed to be represented by a collection of  $n$  oscillators with frequencies  $\omega_j$ , damping  $\gamma_j$ , and strengths  $\omega_{pj}^2$ . The multiple harmonic oscillator model (Lorentz model) for such a solid gives a complex dielectric function

$$\epsilon = \epsilon_0 + \sum_j \frac{\omega_{pj}^2}{\omega_j^2 - \omega^2 - i\gamma_j\omega} \quad (4)$$

where  $\epsilon_0$  is the dielectric function at frequencies high compared to the oscillators of concern. Calculation of reflectance

from the complex dielectric function enables one to vary the oscillator parameters until the measured reflectance is well fitted. The oscillator parameters then give the dielectric function variation with frequency, from which optical constants can be calculated. A classic example of work which uses this technique is the determination of optical constants for crystal-line quartz reported by Spitzer and Kleinman (1961). Unfortunately, this technique is not very useful in the case of powdered materials since the Fresnel equation is not well obeyed by these solids, even when compressed into self-supporting tablets.

### C. Small Particle Theory

For the purpose of inverting measurements on small particle systems to infer optical constants it is necessary to have proper equations for relating the measured quantities to the optical constants. The Fresnel equation of the previous section, for example, would not be appropriate. The only general theory for interaction of light with a small particle system is the solution for the electromagnetic boundary value problem for spheres, often referred to as Mie theory after one of its originators, Gustav Mie (1908). The Mie theory is perfectly general in treating any size and any complex refractive index, but only for homogeneous spheres. The solutions are expressed in convergent series form and hence require computer calculations to implement the theory. With the current availability of modern computers and efficient Mie programs it is possible to analyze experiments on tenuous collections of small particles in order to derive optical constants of the solids. An experiment might consist of dispersing the spherical particles as a dilute suspension in air or in an infrared-transparent matrix such as KBr, measuring wavelength dependent extinction (scattering + absorption), and fitting the measurements by means of Mie theory with dielectric functions described (for example) by the

Lorentz oscillator expression (4). Logical normalization for the measured extinction is per unit mass or per unit volume of particulate, these two differing only by the density of the solid material.

Two serious problems face the experimenter wishing to obtain optical constants in this way, however. First, the extinction normalized per unit volume of solid is a strong function of size for particle sizes commonly found in powdered materials. (See Day et. al., 1974, for examples of this.) Consequently, the particle size distribution would have to be accurately determined and used in the Mie calculations before accurate optical constants results could be expected. There is a fairly simple experimental way around this problem, however. If a small sized fraction of the original powder is segregated, the volume-normalized extinction becomes constant for given index of refraction, independent of size. The upper limit on particle size necessary to achieve this simplification is about  $1\text{ }\mu\text{m}$  for most highly absorbing materials in the  $10\text{ }\mu\text{m}$  infrared region, as explained in the previous report (Huffman, 1979). The extinction measurements on a sub-micrometer fraction of powder dispersed in transparent material could thus be inverted to yield optical constants without knowing anything further about the size distribution.

The other major problem with this plan is that most particulate systems contain nonspherical shapes which are not correctly treated by Mie theory. Contrary to much common opinion on the subject small particle extinction (even in the small particle Rayleigh limit) can be highly shape-dependent. The problem is illustrated dramatically in the upper part of figure 1 where extinction for spheres calculated with accurately measured bulk optical constants for  $\alpha\text{-Al}_2\text{O}_3$  is compared with volume-normalized extinction measured for a sub-micrometer fraction of aluminum oxide particles. The

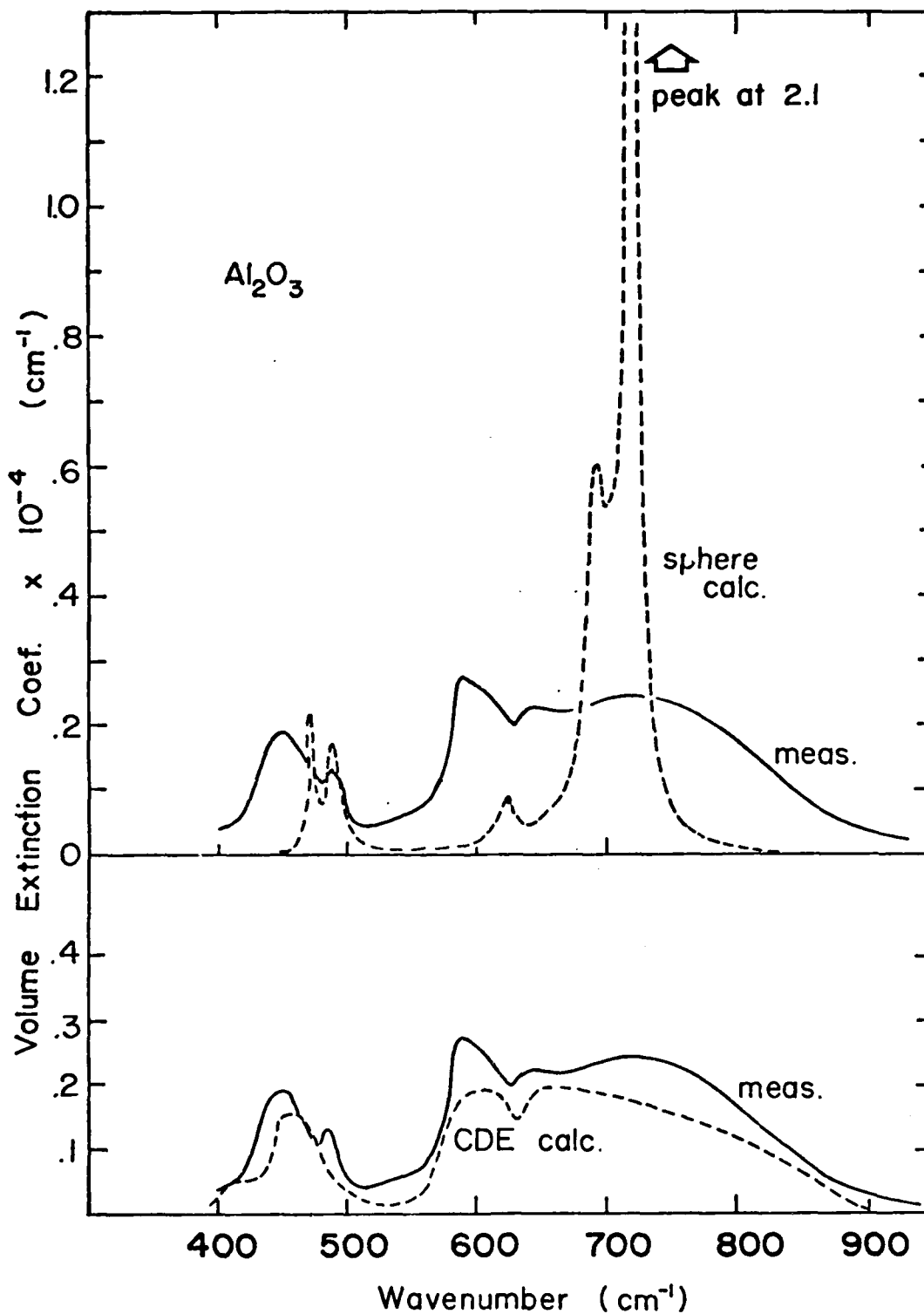


Fig. 1: Volume-normalized extinction measured for  $0.3\text{ }\mu\text{m}$  particles of  $\alpha\text{-Al}_2\text{O}_3$  (solid curves) compared with calculations (dashed curves) using measured bulk optical constants.  
 (a) Upper figure - the calculations are for spheres.  
 (b) Lower figure - the calculations are for a continuous distribution of ellipsoidal shapes in the Rayleigh approximation.

particulate sample is comprised of a small quantity of high quality alumina powder ( $\alpha\text{-Al}_2\text{O}_3$ ) from Buehler Company having an average size of  $0.3\text{ }\mu\text{m}$ , dispersed in transparent KBr as described in Section IV. Dielectric functions relative to the dielectric function of the KBr matrix have been used in the calculations. No adjustable parameters have been used in the comparison. The serious lack of agreement between calculations and measurements, we are convinced, is due to the effect of nonspherical particles which are not adequately described by the sphere theory.

Our solution to the problem of treating nonspherical particle extinction has been to develop a simple theory that provides a much improved description of extinction by a wide distribution of particle shapes (Huffman and Bohren, 1980). The theory treats the shape distribution by means of a random distribution of ellipsoidal shapes in the Rayleigh approximation. The simple resulting expression for absorption cross section  $C_{\text{abs}}$  normalized per unit volume of solid  $v$  for a random distribution of all possible ellipsoidal shapes is

$$\langle\langle C_{\text{abs}} \rangle\rangle = kv \text{Im} \left\{ \frac{2\epsilon}{\epsilon - 1} \text{Log } \epsilon \right\} \quad (5)$$

where  $k = 2\pi/\lambda$  is the wave number in the medium surrounding the particles, and Log denotes the principal value of the complex number. An example of the much improved agreement of this new theory with measurements for quartz particles has been published (Huffman and Bohren, 1980) in the proceedings of the Albany conference on light scattering by irregular particles. A new comparison of extinction measurements and calculations for  $\text{Al}_2\text{O}_3$ , shown at the bottom of figure 1 clearly shows the superiority of the ellipsoidal shape distribution theory over the sphere theory of the upper part of the figure. Again no arbitrary normalization has been applied to either theory or experiment.

### III. EXPERIMENTS ON PARTICLES OF SPECIFIC SHAPE

In the previous section we have given a simple theory for extinction by a wide distribution of particle shapes and have shown that the theory gives an accurate description of the extinction spectrum of irregular quartz and aluminum oxide particles. There is a prevalent school of thought that ascribes the large differences between measured and calculated extinction (usually assuming spheres), such as one sees in the  $\text{Al}_2\text{O}_3$  comparison of figure 1a, to a variation of optical constants with particle size. This could of course explain the lack of agreement, but it would invalidate the entire concept of optical constants as the basic summary of optical properties of matter as applied to small particles. Now it must be acknowledged that there must be some size at which bulk optical constants break down as one successively subdivides matter into ever smaller pieces. The proof of this is that optical spectra of solids bear little resemblance to the optical spectra of the atoms and molecules out of which the solid is composed. There are a few well documented cases in which optical constants vary appreciably with size. One involves the limitation of mean free path of electrons in metals by the boundaries of the particle (see Huffman, 1977, for references to this effect). Such effects only become appreciable for particle sizes of about  $100 \text{ \AA}$  or less. For particles in the range from 0.1 to  $1.0 \text{ \mu m}$  characteristic of this study, one needs to be convinced that optical constants have not changed appreciably from those of bulk material.

In order to clearly separate effects due to varying particle shape and due to altered optical constants, both of which may give rise to discrepancies between sphere theory and measurements, we have put considerable effort into producing particle ensembles of fixed shapes -- one system of spheres and one system of cubes. If the measured extinction for these particles when well isolated from one another agrees



with calculations assuming bulk optical constants we would infer that the bulk optical constants are adequate, i.e. they have not changed in the small particles.

Silica smoke spheres Small, solid spheres are not, as a rule, easily generated; an exception is  $\text{SiO}_2$  smoke, which can be produced readily enough by striking an arc (ac or dc) in air between silicon electrodes or carbon electrodes embedded with pieces of silicon or quartz. These smokes consist of nearly perfect spheres of amorphous  $\text{SiO}_2$  with diameters in the range between about 100 Å and 1000 Å; they satisfy the requirements of being spherical, isotropic, composed of material with accurately measured infrared optical constants, and well within the range where volumetric extinction is independent of size. The biggest problem to be overcome is that upon formation in air the spheres link together in clusters and chains which, in electron micrographs, resemble strings of pearls. Steyer, et. al. (1974) published infrared extinction data on this system of particles because of its approach to ideality; however, they found a factor of 2.2 between calculated and measured peak extinction. In the present work we have undertaken a more concerted effort to disrupt clusters and produce isolated spheres in a KBr matrix. Results of the newer experiments are shown in figure 2 where measured extinction is compared with that calculated from sphere theory with no adjustable parameters. Bulk properties used in the calculations were taken from the paper by Steyer, et. al, which agree well with independent measurements reported by Zolotarev (1970) and by Neoroth (1955). Evidence that the silica spheres have been dispersed more than in earlier efforts is that the discrepancy between measured and calculated peak extinction has been reduced from a factor of 2.2 to about 30%. We feel that the remaining discrepancy between sphere calculations and measurements can be attributed to residual clumping of particles, which causes slight broadening of the small-particle

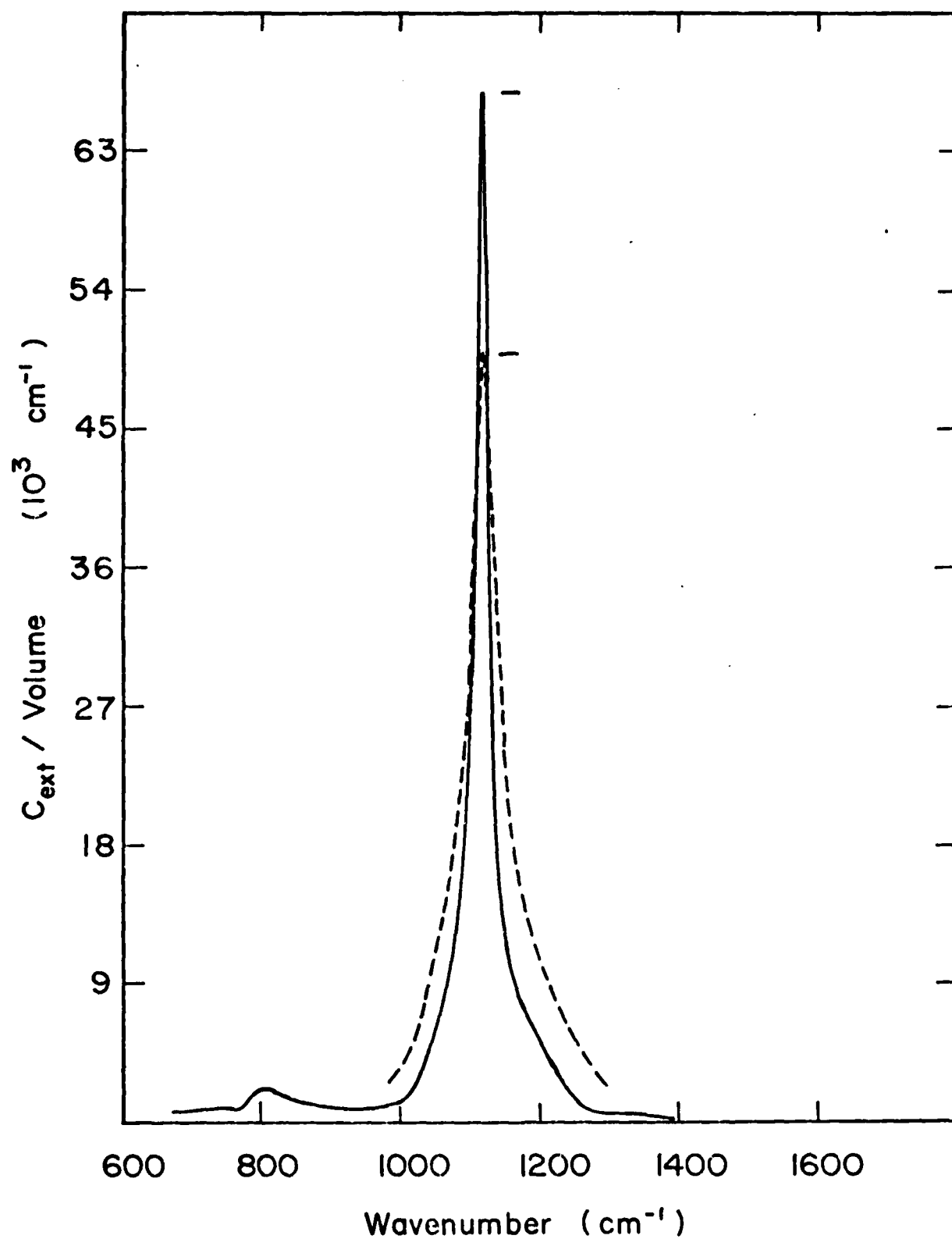


Fig. 2: Volume-normalized extinction for fused quartz smoke particles measured by the KBr pellet technique (dashed line) and calculated (solid line) assuming spheres and measured bulk optical constants.

absorption bands at the expense of decreased peak height. Even without invoking such residual clumping, however, the comparison based on bulk optical constants seems favorable: the predicted absorption band position and shape is very close to that measured. In view of possible experimental uncertainties in the bulk dielectric function, the agreement is sufficiently close to convince us that, in this instance at least, bulk optical constants are appropriate to particles averaging less than  $0.1 \mu\text{m}$  in diameter.

Magnesium oxide cubes One other specific shape for which exact calculations (in the small particle limit) have been published is the cube. Fuchs (1978,1975) derived an expression for absorption by cubes in the electrostatics approximation (equivalent to the Rayleigh limit) and compared his results (Fuchs, 1974) with results of lattice dynamical calculations of Chen, et. al. (1978) for an MgO microcrystal of 900 atoms ( $10 \times 10 \times 9$ ). There was good agreement between the two theories even for this small number of atoms. Possibly no other solid has been studied so much for the purpose of understanding small particle infrared absorption modes as MgO, which characteristically forms cubes when produced in the usual manner from burning magnesium ribbon. Experimental work on infrared absorption by MgO smoke has been reviewed by Genzel (1975). Discrepancies between measured extinction and calculations (assuming spheres again) led to the conclusion that bulk optical constants must be modified in certain ways. Because of this conclusion we have carefully redone the experiment taking great care to disperse the chains of cubes into isolated particles in the KBr matrix, following techniques similar to those used for the silica smoke.

Results of the measurements are shown in figure 3, where the particles are successively more dispersed as one progresses downward on the figure. Dashed curves are theoretical calculations based on the bulk optical constants measured by Jasperse,

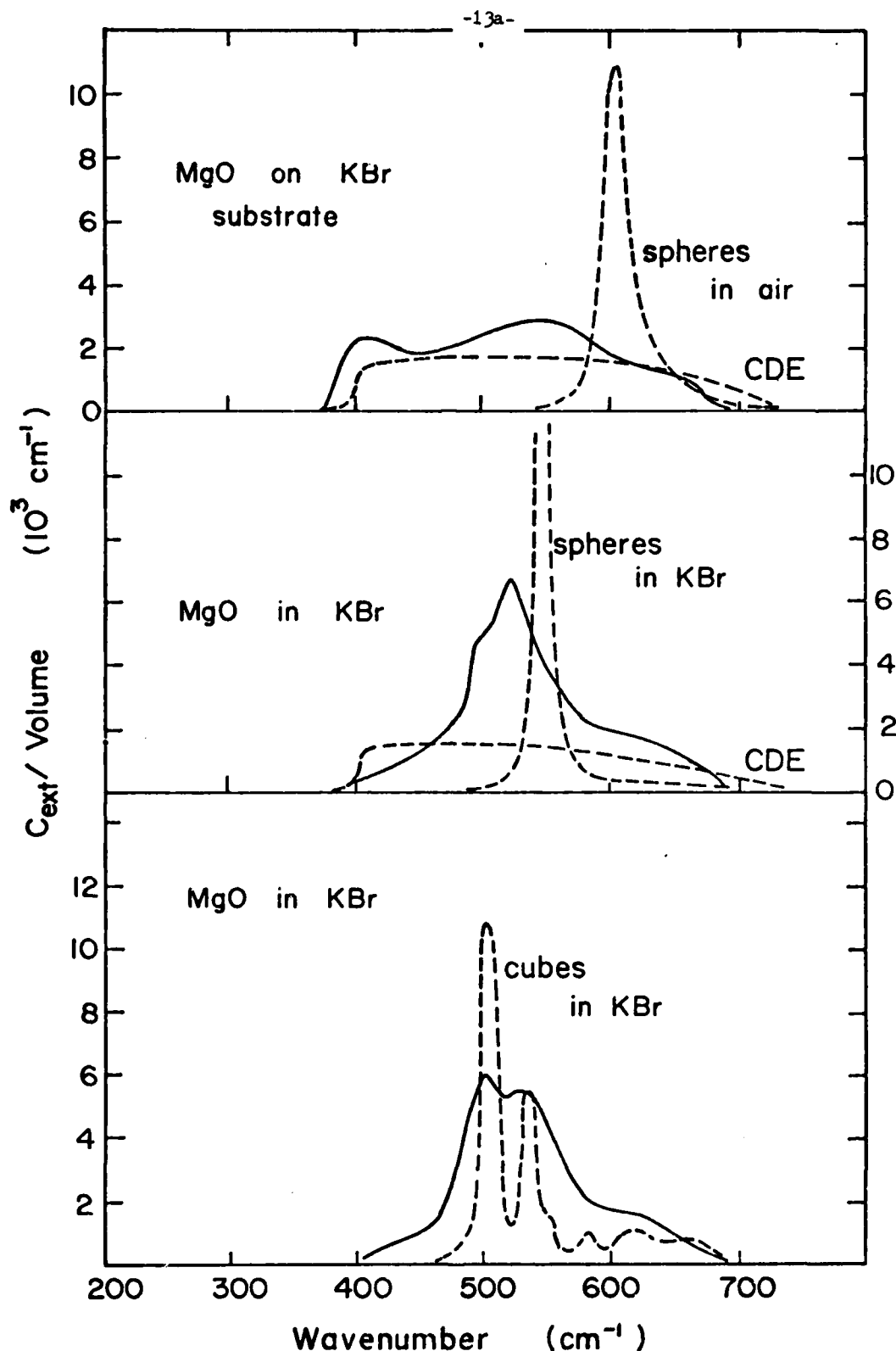


Fig. 3: Volume-normalized extinction measurements (solid curves) and calculations (dashed curves) for MgO smoke particles in different degrees of dispersal. Upper curve (a): Smoke loosely collected on a substrate compared with sphere calculations and CDE calculations assuming a surrounding medium of air with  $\epsilon_m = 1$ . Middle curve (b): Smoke dispersed by agitating for several hours in KBr powder. Lower curve (c): Smoke dispersed by agitating for several days in KBr powder. Note the apparent development of the cube modes as the MgO particles are more effectively segregated into single particles.

et. al. (1966). In the upper part of the figure volume-normalized extinction is shown for a sample prepared by burning magnesium ribbon in air and collecting the particles on a clean KBr pellet. The middle curve is for the same smoke but dispersed by grinding with KBr and shaking the mixture for three hours in a glass vial with steel balls before pressing a pellet; the bottom curve is for a similarly prepared sample, but shaken for three days before pressing a pellet.

Particles dispersed on the KBr substrate are not strictly isolated, and perhaps this should be taken into account by basing calculations on the Maxwell-Garnet theory (or a similar theory) as Genzel and Martin (1972, 1973) did. However, the particle volume fraction is small, so we are not misrepresenting the experiment too badly by comparing it with calculations for isolated spheres and a continuous distribution of isolated ellipsoids.

Comparison of measurements for particles dispersed on and in KBr is quite revealing. The extinction curve for particles on a KBr substrate shows a peak at approximately  $400\text{ cm}^{-1}$ , the transverse optical mode frequency for bulk MgO. This feature has been observed a number of times, and it is discussed in some of the references already cited. Its explanation now appears to lie in a selective shape effect caused by the tendency of MgO cubes to link together into chains, which are more closely approximated as cylinders or elongated spheroids than spheres. A similar effect was observed in NiO smoke particles by Hunt, et. al. (1973), who analyzed their results on the basis of calculations for cylinders as well as spheres. Further evidence that the chain formation is responsible for the  $400\text{ cm}^{-1}$  bump is that it disappears upon thorough dispersal of the particles in KBr (middle and lower sections of the figure); this effect was pointed out by Dayawansa and Bohren (1978).

In the middle curve of figure 3 sphere and CDE calculations are compared with measurements on MgO cubes well dispersed in KBr: neither is very satisfactory. The sphere calculations peak fairly close to the measured peak, but not coincident with it; the CDE calculations show appreciable absorption over approximately the same frequency range as the measurements, but no structure. If the optical constants we have used are appropriate to the smoke particles, figure 3b suggests that neither spheres nor a broad distribution of shapes are good approximations for MgO particles. This is hardly surprising since electron micrographs reveal that MgO smoke is comprised of cubes.

Fuchs (1975) has presented results from his calculations for ionic crystal cubes in the form of strength factors  $C(j)$  and  $L(j)$ 's, which are geometrical factors related to the lengths of major axes in small ellipsoid theory. His result for volume-normalized absorption (absorption = extinction in this limit) is

$$\alpha = k \operatorname{Im} \sum_j \frac{C(j)}{\frac{\epsilon_m}{\epsilon - \epsilon_m} + L_j} \quad (6)$$

where  $\sum C(j) = 1$  for a sum over all modes. This can be compared with the absorption by an ellipsoid in the electrostatics approximation (Huffman and Bohren, 1980)

$$\alpha = k \operatorname{Im} \sum_1^3 \frac{1/3}{\frac{\epsilon_m}{\epsilon - \epsilon_m} + L_j} \quad (7)$$

We have used dielectric functions  $\epsilon$  calculated from the

oscillator parameters for bulk MgO determined by Jasperse et. al. (1966) along with the wavelength dependent (real) dielectric function  $\epsilon_m$  for the KBr matrix as given by June (1972), to calculate the expected absorption spectrum of MgO cubes. Comparison of these theoretical results with the experimental results on well dispersed MgO smoke shown in figure 3c is now rather interesting. One might imagine that the data contain an underlying background extending from about  $400\text{ cm}^{-1}$  to about  $700\text{ cm}^{-1}$ , perhaps similar to our CDE results. In addition it appears that the experiment is resolving the two strongest cube modes near  $500$  and  $530\text{ cm}^{-1}$ . A clear resolving of these modes has not previously been made in experimental data. If the two modes are indeed being resolved, it implies the important fact that the widths of the individual cube modes are not too much greater than the width of the dominant bulk absorption band. Genzel and Martin (1972) used an eight-fold increase in the damping factor and Fuchs (1975) invoked a factor of 2.5. Such enhanced damping suggested by the broad and featureless nature of the previously published extinction curves for MgO does not seem to be necessary now in view of the apparent resolution of individual cube modes. The MgO results along with the favorable comparison of experiment and theory for silica spheres (figure 2) implies that bulk optical constants do not have to be appreciably modified, as by increasing the damping factor for infrared modes of particles, even for particles in the  $100\text{ \AA}$  to  $1000\text{ \AA}$  size range.

A far greater proportion of the present contracted research has been spent on the material contained in this section than was originally planned, at the cost of our not being able to do optical constants determinations on as many new solids (section V). The justification for this has been that there has not been nearly enough understanding of the role of shape effects

in the infrared spectra of particulates having strong absorption features. Unfortunately, the more we understand, the more difficult the optical constants determinations have become.

#### IV. SUMMARY OF EXPERIMENTAL TECHNIQUES USED

In this work so far we have eliminated size dependence by considering only Rayleigh particles, but we have added the complexity of shape dependence. This gives rise to a serious problem since most particles cannot be produced in a specific shape. Particles more likely have some wide distribution of shapes. Even spherical smoke particles, we have seen, quickly agglomerate into irregular bundles having effective irregular shapes. It is because of the fact that heterogeneity of shape is more common than homogeneity of shape that the theory we have most often chosen to apply in deriving optical constants from measurements is the random distribution of shapes as modeled by Rayleigh ellipsoid theory.

Because of the difficulties and uncertainties still present in extracting optical constants from powdered materials, and because optical constants of powders are identical to those of the bulk solid (as we have argued in the preceeding section), it is desirable to continue doing some optical constants determinations on powders ground from the solids. We will therefore summarize our techniques used, both for the bulk solid samples and for the powders.

##### A. Bulk Solids

In spectral regions of relative transparency for solids, a combination of reflectance and transmittance through a polished slab permits one to easily determine both optical constants at any wavelength. In spectral regions of most interest in this work, specifically in regions near strong infrared resonances, absorption is so great that no measurable



light passes through even the thinnest mechanically polished slices. One must rely on reflectance measurements. But reflectance over a range of wavelengths must be analyzed since one measurement at each wavelength cannot determine two optical constants. The two ways of analyzing the reflectance data are the Lorentz oscillator fit and the Kramers-Kronig analysis.

Homogeneous, bulk samples such as single crystals or glassy solids are cut with a diamond saw into convenient-sized slabs of about 10 mm x 5 mm x 1 mm. One side of the slab is polished by conventional techniques appropriate to the given sample. Silicate samples such as obsidian are sawed and ground to size, then lapped and polished with successively finer diamond grit (45  $\mu\text{m}$  to 1/4  $\mu\text{m}$ ) on plexiglass, followed by a final polish with alumina if necessary. A good quality optical surface in visible light insures that the sample is quite smooth compared to the infrared light. Almost-normal-incidence reflectance measurements are made using a beam condensing reflectance attachment in a Perkin Elmer dual beam infrared spectrophotometer, with a freshly evaporated thick aluminum film on glass as the reflectance standard. One example of resulting reflectance spectra is shown in figure 5 where reflectance measured for the volcanic glass obsidian is shown. If the spectral range of reflectance measurements is limited (to a region from 5 to 15  $\mu\text{m}$  for example) the Lorentz multiple oscillator equations are used to compute dielectric functions by equation (4),  $n$  and  $k$  are determined from (2), and the reflectance calculated from the Fresnel equation (3). With a FORTRAN program for doing this on an interactive computer, oscillator parameters are chosen and varied until a satisfactory fit is achieved, from which the spectrum of optical constants is produced. When a broad spectral range of reflectance measurements has been taken the more direct process of inverting the data by means of Kramers-Kronig analysis is done. An excellent example of this technique is found in the paper by

Spitzer and Kleinman (1961).

## B. Powder Samples

Our technique for determining optical constants of powdered materials is analogous to the bulk reflectance technique in which measurements are fitted with a Lorentz multiple oscillator model. In the case of powders the measurements are extinction measurements, and the theory for shape dependent extinction replaces the Fresnel equation for bulk reflectance. There are several experimental constraints that must be imposed on the sample, however, to insure that the theory applies to the measurements. The constraints are that the particles be small (normally sub-micrometer), well isolated from one another, and that the total mass of particles be accurately known. If the random shape distribution theory is used, the particles should also be of irregular shape as normally produced by crushing and grinding.

The experimental procedure, briefly, is to grind the solid material to a fine powder, if it is not already in such form and segregate a sub-micrometer fraction by settling in an air chamber for an appropriate length of time as determined by Stokes' law of settling. The remaining suspended particles are collected by pumping out the supporting gas through a membrane filter. The collected particles are then weighed on a balance sensitive to 1 microgram, dispersed in powdered, spectroscopic grade KBr powder, and pressed into infrared-transparent pellets of 1/2 inch diameter using a force of 20,000 lbs in an evacuable pressure cell. The clear KBr pellets containing the dilute, dispersed sample are placed in the sample cell of the infrared spectrophotometer for transmission measurements. Masses per unit cross sectional area of 0.1 to 0.5 mgm/cm<sup>2</sup> are normally appropriate for the strong absorbers of concern here.

Extinction  $\alpha$  normalized per unit volume of the sample

is calculated from the equation

$$\alpha = \frac{\rho}{\sigma} \ln 1/T$$

where  $\sigma$  is the mass of sample per unit area,  $\rho$  is the bulk density of the solid, and  $T$  is the spectral transmittance. The resulting extinction spectrum  $\alpha(\omega)$  or  $\alpha(\lambda)$  is compared with calculations for irregular particle extinction in the Rayleigh approximation (CDE) using equation (5) for extinction with equation (4) representing the dielectric functions of the powder relative to the matrix. This procedure has been previously evaluated by applying it to several solids including quartz, NiO,  $\text{CaCO}_3$ , and SiC, for which accurately measured optical constants have been available for single crystals (Huffman, 1979). Although reasonably favorable comparisons were achieved, we have continued to evaluate the process by comparing optical constants derived from the small particles and from the bulk samples.

### C. Accuracy of Measured Optical Constants

Because of the somewhat indirect way in which optical constants are derived, for bulk samples as well as for small particle samples, it is difficult to assign uncertainties to the results, and uncertainties are usually not cited in such work. Unfortunately, workers in applied fields often tend to take the "measured" optical constants as being perfectly accurate, since no error bars are given. Even in the much-used bulk techniques, however, results on single crystal bulk solids from different investigators show large discrepancies. In order to show this and to give some feeling for what constitutes "good agreement" in the very difficult game of

infrared optical constants determinations, we have considered the case of magnesium oxide. MgO has been commercially available for many years in the form of pure single crystals which can be easily cleaved to produce atomically smooth surfaces for reflectance spectroscopy in the infrared. The infrared optical constants of MgO have thus been determined by several investigators. In search of the best published optical constants for calculations to relate to our own small particle extinction measurements (section III) we have looked critically at three different sets of experimentally determined dielectric functions. The results are compared in figure 4. References are given in the figure caption. The lack of agreement clearly shows the difficulty in accurately determining the spectrum of wavelength-dependent optical constants in the region of strong absorption and dispersion associated with crystal lattice vibration bands. The comparison of MgO results for bulk single crystals in figure 4 puts into perspective our own efforts in the more difficult determinations of optical constants of particulate systems.

## V. EXPERIMENTAL RESULTS

In this section we present the results of optical constants determinations for powdered materials we have studied along with optical constants determined from some bulk solids from which the samples came. In cases where the results were derived using Lorentz oscillator theory the resulting oscillator parameters are given. Optical constants and dielectric functions can be calculated from equations (4) and (2), along with any other desired optical properties such as transmission and reflectance from a slab of the material. This appears to be the most efficient way to transfer the information to the reader. Oscillator parameters have been collected in the Appendix for convenience. In cases where bulk optical constants

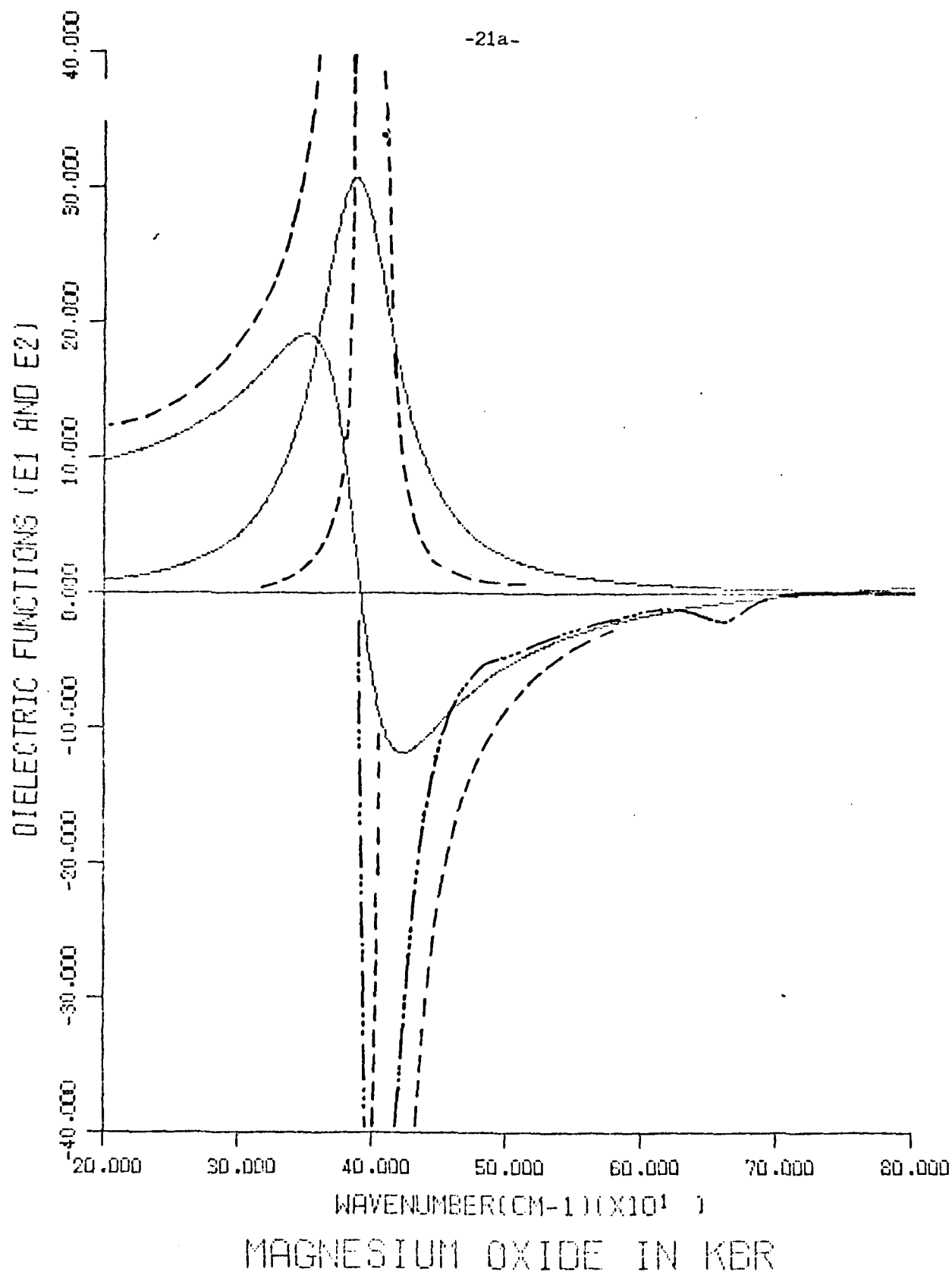


Figure 4: Dielectric functions of bulk, single crystal MgO-  
 "measured" by three different groups. Jasperse et. al. (1966)  
 dashed curves. Häfele et. al. (1963) - dash-dot curves. Dowling  
 and Randall (1977) - full curves.

have been derived from Kramers-Kronig analysis, results are given as graphs of optical constants or dielectric functions.

In the case of three solids in this collection -- chlorite, montmorillonite, and serpentine -- we have taken extinction measurements from the published literature rather than repeating the measurements. In most cases the rather extensive published tabulations of powder extinction spectra are of little value for the purpose of extracting optical constants, since a sufficiently small-size fraction of particles was not segregated for measurement. An exception to this is the work of Dorschner, et. al, (1978) who reported extinction measurements similar to ours for the silicate minerals talc, chlorite, montmorillonite, and serpentine. Because these authors were interested in applications involving interstellar grains, which are sub-micrometer particles in interstellar space, they were careful to select only the very small sizes. Although we have repeated their experiments on talc, there seemed to be no good reason for repeating measurements on the other powdered solids. Hence we have analyzed the results of Dorschner et. al. with our technique and presented the results for chlorite, serpentine, and montmorillonite in this section.

#### A. Obsidian

Obsidian is a glassy (amorphous) solid of volcanic origin which is primarily a mixture of magnesium, aluminum, and calcium silicates with composition varying somewhat from one locale to another. Samples used in this study were from Utah where they were collected as rounded pebbles of about 1 inch diameter. They were chosen because high quality bulk samples could be prepared from them as well as powder samples ground from the bulk material. The comparison of optical constants from the two types of sample provides a further indication of the degree to which optical constants can be derived successfully

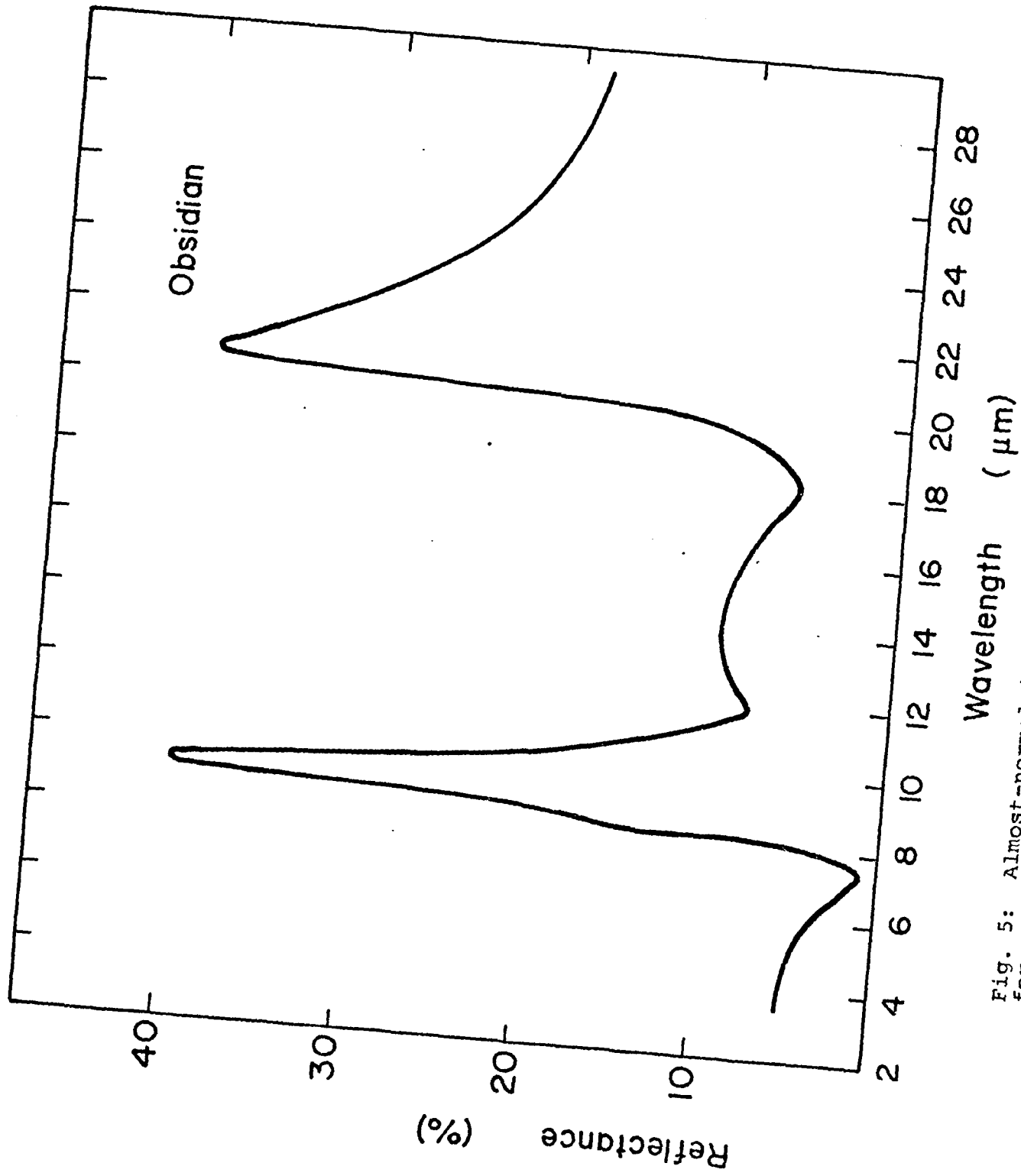


Fig. 5: Almost-normal-incidence reflectance spectrum measured for a polished bulk slab of obsidian from Utah.

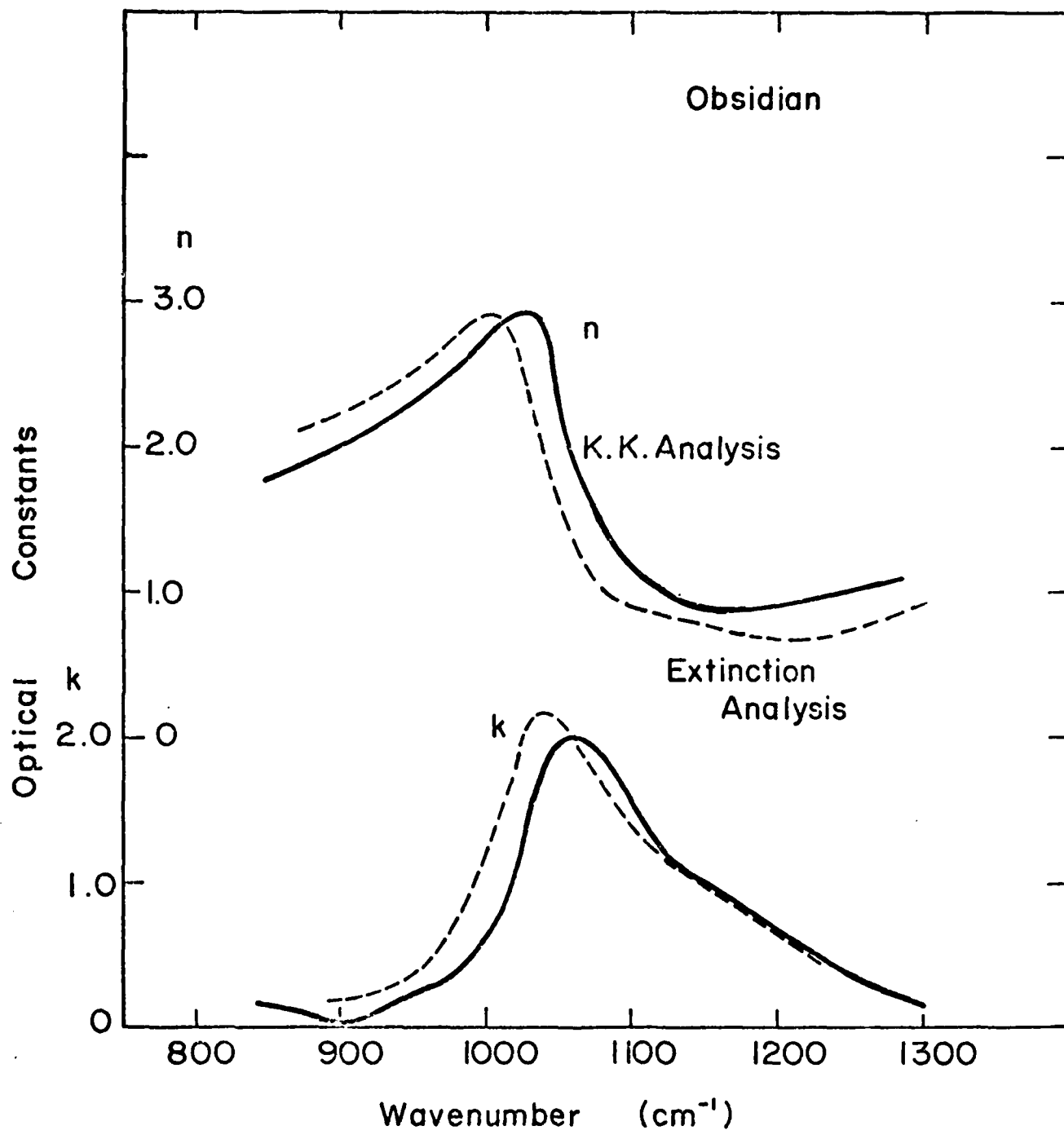


Fig. 6: Optical constants of obsidian derived from Kramers-Kronig analysis of the reflectance data (solid curves) from fig. 5 and derived from an oscillator fit to the small particle extinction data (dashed curves).



from powdered materials.

Optical constants determinations were made on polished samples of the bulk material by measuring almost-normal-incident reflectance from about 2  $\mu\text{m}$  to about 40  $\mu\text{m}$  wavelength and analyzing by means of the Kramers-Kronig technique. The reflectance measurements are shown in figure 5 and the derived optical constants are shown in figure 6 as the solid lines. Optical constants determined from extinction measurements on the powdered obsidian are shown as the dashed curves in figure 6, with Lorentz oscillator parameters listed in the Appendix. The comparison of optical constants in figure 6 gives an idea of how reliable the small particle technique may be. Although there is a small displacement of the main absorption band, as signified by the peak of the  $k$  curve, the comparison is considered to be favorable, especially compared to discrepancies such as are commonly present in different single crystal measurements (see figure 4).

#### B. Serpentine

Serpentine is not strictly a single mineral but is usually a mixture of several similar hydrous magnesium silicates such as antigorite and chrysotile, both having a chemical formula of  $\text{H}_4\text{Mg}_3\text{Si}_2\text{O}_9$ . Since serpentine is not available in homogeneous bulk form, it is an excellent example of the need for the present work. On the other hand, since it is not an isotropic, single component mineral, the optical constants results should be looked upon with some caution (see the remarks in the closing section of this report). Since Dorschner et. al. (1978) appear to have done an adequate job of segregating the small particle fraction and making extinction measurements in the same way as we do, we have elected to use their published extinction results. The volume-normalized extinction data and the theoretical fit using

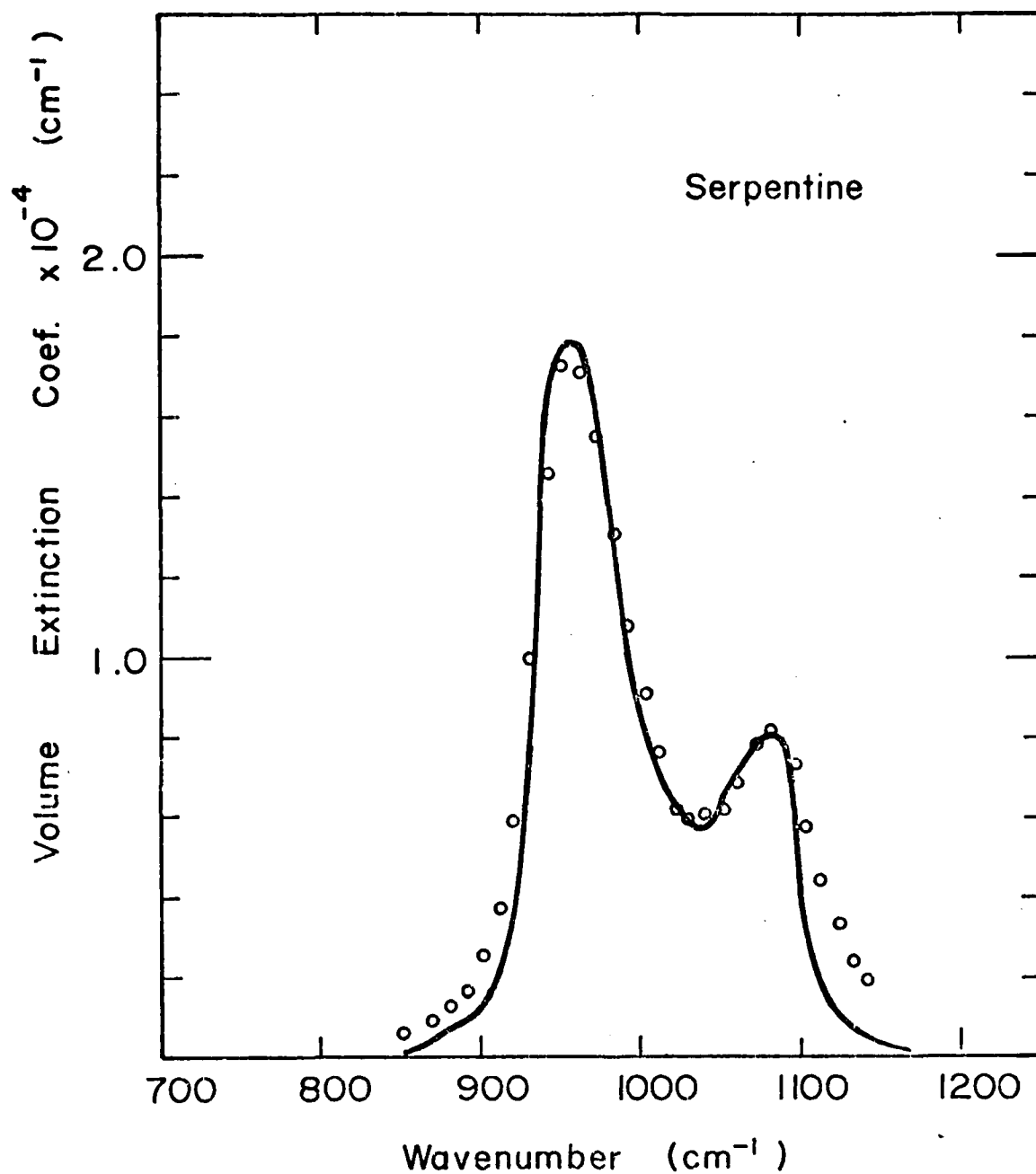


Fig. 7: Volume-normalized extinction measured for a small size fraction of serpentine (solid curve) compared with the theoretical fit (circles) used to infer optical constants.

our CDE calculations are shown in figure 7. Oscillator parameters derived from the fit, which can be used to generate optical constants in this spectral region are listed in the Appendix.

### C. Chlorite

Chlorite is a mixture of magnesium and aluminum silicates with water. The extinction data from Dorschner et. al. were easily fitted in this case with a one oscillator model to the degree shown in figure 8. To illustrate a representative spectrum of dielectric functions we have included a plot of  $\epsilon_1$  and  $\epsilon_2$  for this case in the frequency region of concern in figure 9. Several points regarding the relationship of small particle extinction spectra to the dielectric function spectra can be illustrated with this example. There is generally an appreciable shift between the small particle absorption and the bulk absorption mode. Note that the extinction peaks at about  $985\text{ cm}^{-1}$  whereas the peak of  $\epsilon_2$  is at  $930\text{ cm}^{-1}$ . If a theory were used which did not account for this shift in small particle extinction, the dielectric functions extracted using such a theory would be substantially in error, not only in magnitude but also in peak position of  $\epsilon_2$ . The small particle peak actually occurs near the point where  $\epsilon_1$  is minimum. This is because all shapes of particles will have small particle surface modes in the frequency region where  $\epsilon_1$  is negative. Note that  $\epsilon_1$  in figure 9 is negative at about  $980\text{ cm}^{-1}$ , which is just where the measured extinction of chlorite peaks in figure 8. The interested reader may refer to Huffman (1977) for a further discussion of these small particle modes.

### D. Montmorillonite

Montmorillonite is one of the major minerals comprising

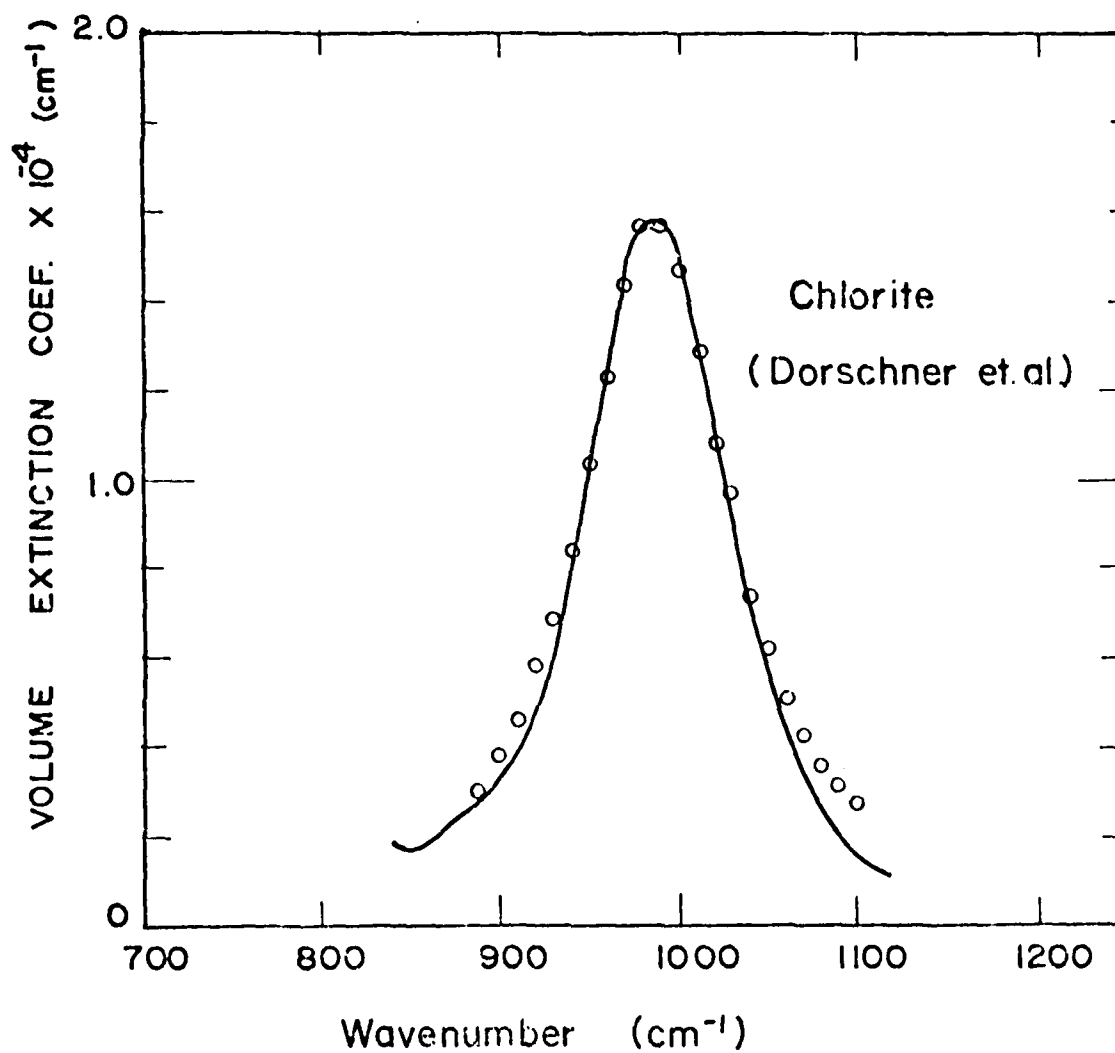


Fig. 8: Volume-normalized extinction measured for a small size fraction of chlorite (solid curve) compared with the theoretical fit (circles) used to infer optical constants.

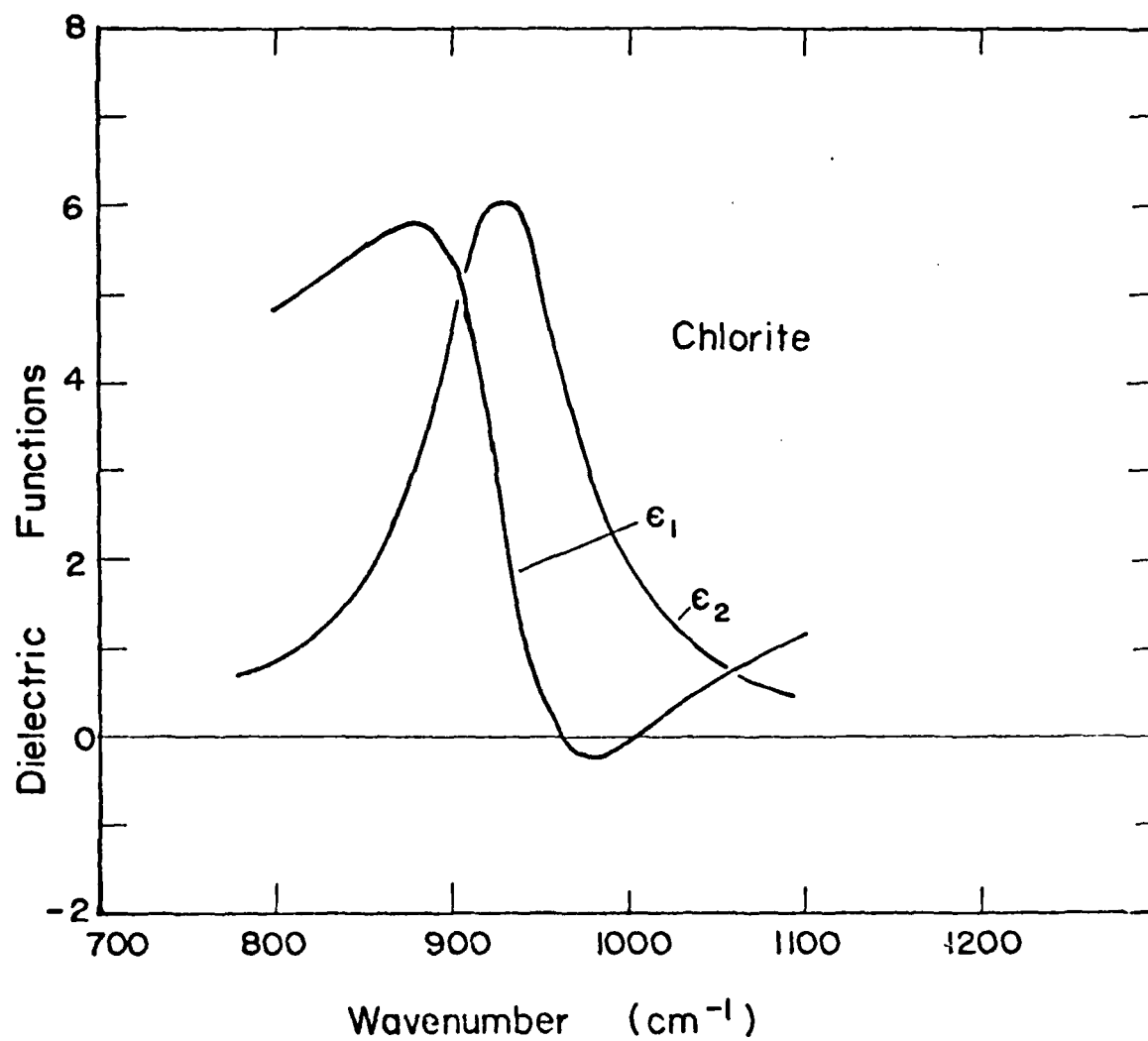


Fig. 9: Dielectric functions for chlorite inferred from extinction measurements and the theoretical fit of figure 8.

various clays. It is a hydrated magnesium-calcium and aluminum silicate which occurs commonly as an alteration product from volcanic ash. In the western United States the common rock bentonite is largely composed of montmorillonite. Lindberg and co-workers (1978) have used montmorillonite as one of the main ingredients in their mixture of minerals put together to mock up atmospheric dust collected in New Mexico and infrared analyzed. The volume-normalized extinction data and the fit for montmorillonite are shown in figure 10b and the oscillator parameters are listed in the Appendix.

#### E. Mt. St. Helens Dust

During the time this work was being carried out, the now-famous explosive eruption of Mt. St. Helens took place, releasing into the atmosphere large quantities of fine dust which greatly affected radiation processes in the atmosphere. This event provided an interesting example of an important aerosol material for which bulk samples were not available, although one might expect a certain optical similarity to the previously studied silicates such as obsidian and montmorillonite. Dust samples taken from the region of Ellensburg Washington, were size-segregated and dispersed in KBr in our usual way and extinction measurements made. The results are shown in figure 10a along with the fit achieved from theory. Oscillator parameters are found in the Appendix.

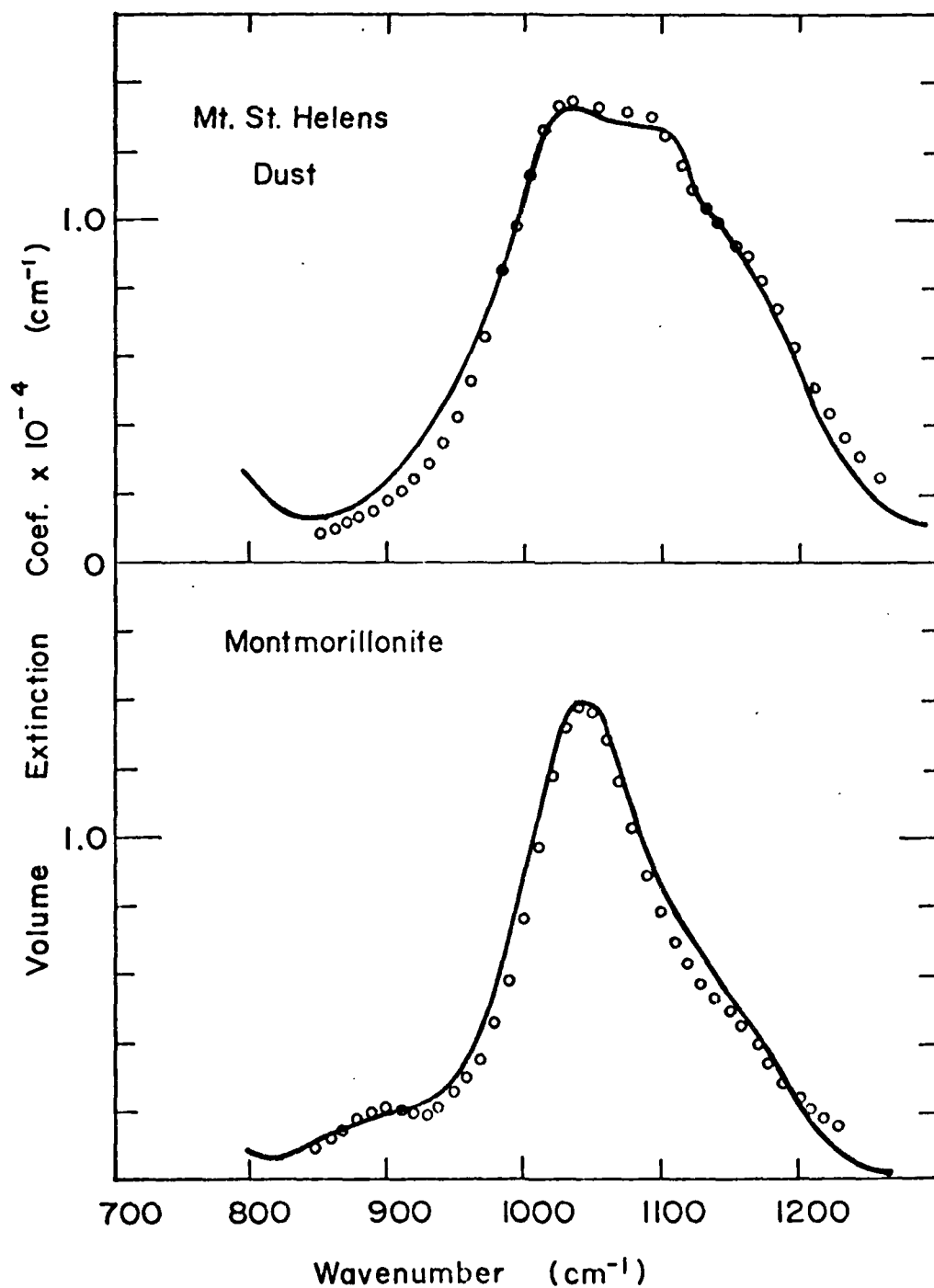


Fig. 10: Volume-normalized extinction measured for small size fractions (solid curves) and compared with the theoretical fits (circles) used to infer optical constants.  
Upper graph 10a: Mt. St. Helens volcanic dust  
Lower graph 10b: Montmorillonite

## F. Talc

Talc is a mineral with chemical composition  $\text{Mg}_3(\text{OH})_2(\text{Si}_2\text{O}_5)_2$  that is mined for various industrial applications including the production of high quality powder (talcum powder). The crystal structure of talc is a complicated layer-lattice, monoclinic structure that is highly anisotropic in its physical properties. It has not been found or produced in single crystals of any appreciable size and there are consequently no measured bulk optical constants in the  $10\ \mu\text{m}$  infrared region. During last year's search for the most efficient absorber of single frequency (laser) radiation it was realized that talc has the highest volume-extinction peak of any solid we know of in the  $10\ \mu\text{m}$  region. Because of this fact and the resulting experimentation by other groups interested in the maximum extinction problem it was imperative that we attempt to derive optical constants for talc. In fact, this substance was the main reason we have tried to develop the optical constants determination technique for powders. The very strength of the extinction band portends great difficulty in inverting the experimental data, however, since shape effects always become more serious in the region of the strongest resonances. The other problem that causes much anguish is the crystalline anisotropy which is extreme for talc. Thus talc is both the most interesting and the most challenging of the powdered solids we have dealt with in this work.

Our extinction measurements made on predominately sub-micrometer talc particles segregated by settling in air and dispersed in KBr are shown as the solid lines in figure 11. There is a rather serious disagreement between these measurements and those of Dorschner et. al. (1978) who found a peak extinction of about  $2.1 \times 10^5\ \text{cm}^{-1}$  compared to our maximum of  $6.5 \times 10^4\ \text{cm}^{-1}$ . Our measurements are in reasonable agreement with determinations by Carlon (1980) for talc particles



suspended in air, although there is a small difference to be expected from the different surrounding media (air and KBr) in these two situations. The large discrepancy in comparison with Dorschner et. al. remains a mystery although it could be associated with differing shapes of particles in the two cases. Since we have found the Dorschner measurements to be reliable in other cases, we see no reason to ascribe the difference to procedural errors on their part.

Because talc is such a soft mineral (it serves to define the softest point on Mohs' hardness scale) the powder can be compressed into a pellet close to bulk density with the same technique used to press the KBr pellets. This is the only sample powder in this study soft enough to permit such bulk samples to be produced. Conventional reflectance measurements taken on a pressed talc sample are shown as the solid lines in figure 12. Although we hold some reservations about analyzing this type of experiment, we have nevertheless fitted the measured reflectance to achieve the match shown by circles. The resultant oscillator parameters are given in the Appendix.

The first indication of difficulty in analyzing our extinction data for optical constants was that no fit could be achieved to the extinction data of figure 11 using the distribution of ellipsoids theory. The maximum extinction we could achieve was about  $3 \times 10^4$ . This suggested that only one dominant shape might be involved. Assuming this shape to be spheres it was possible to fit the data, but the results were in substantial disagreement with oscillator parameters from the reflectance fit. The nature of the discrepancy was a serious and unacceptable shift of the dominant oscillator frequency between the reflectance fit and the extinction fit. Results of this dilemma were reported in the third quarterly progress report for this contract, dated June 26, 1980. The problem may lie in the fact that talc particles have one

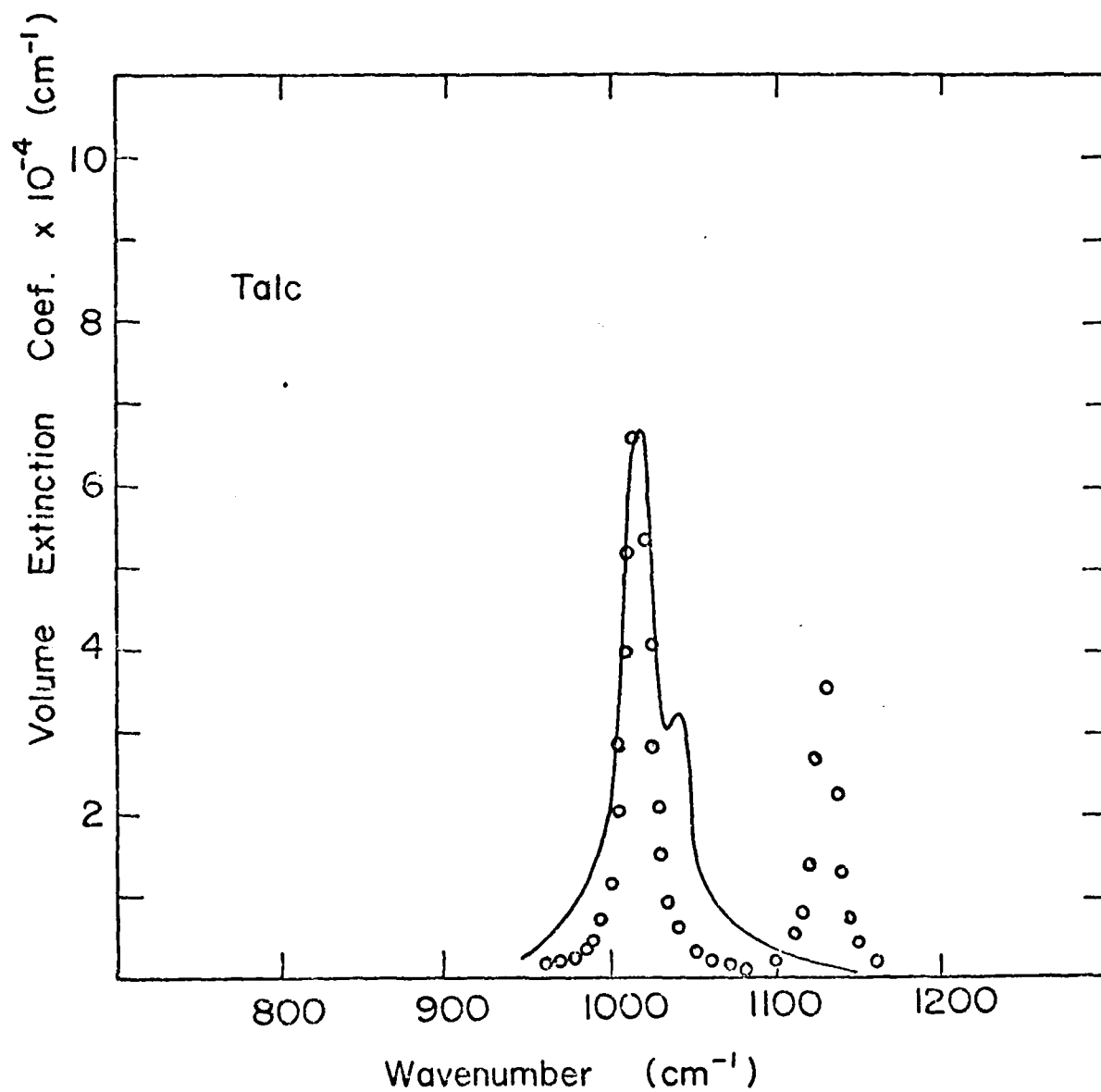


Fig. 11: Volume-normalized extinction measured for talc powder dispersed in KBr (solid line) compared with calculations to fit the main peak assuming a single highly flattened ellipsoid.

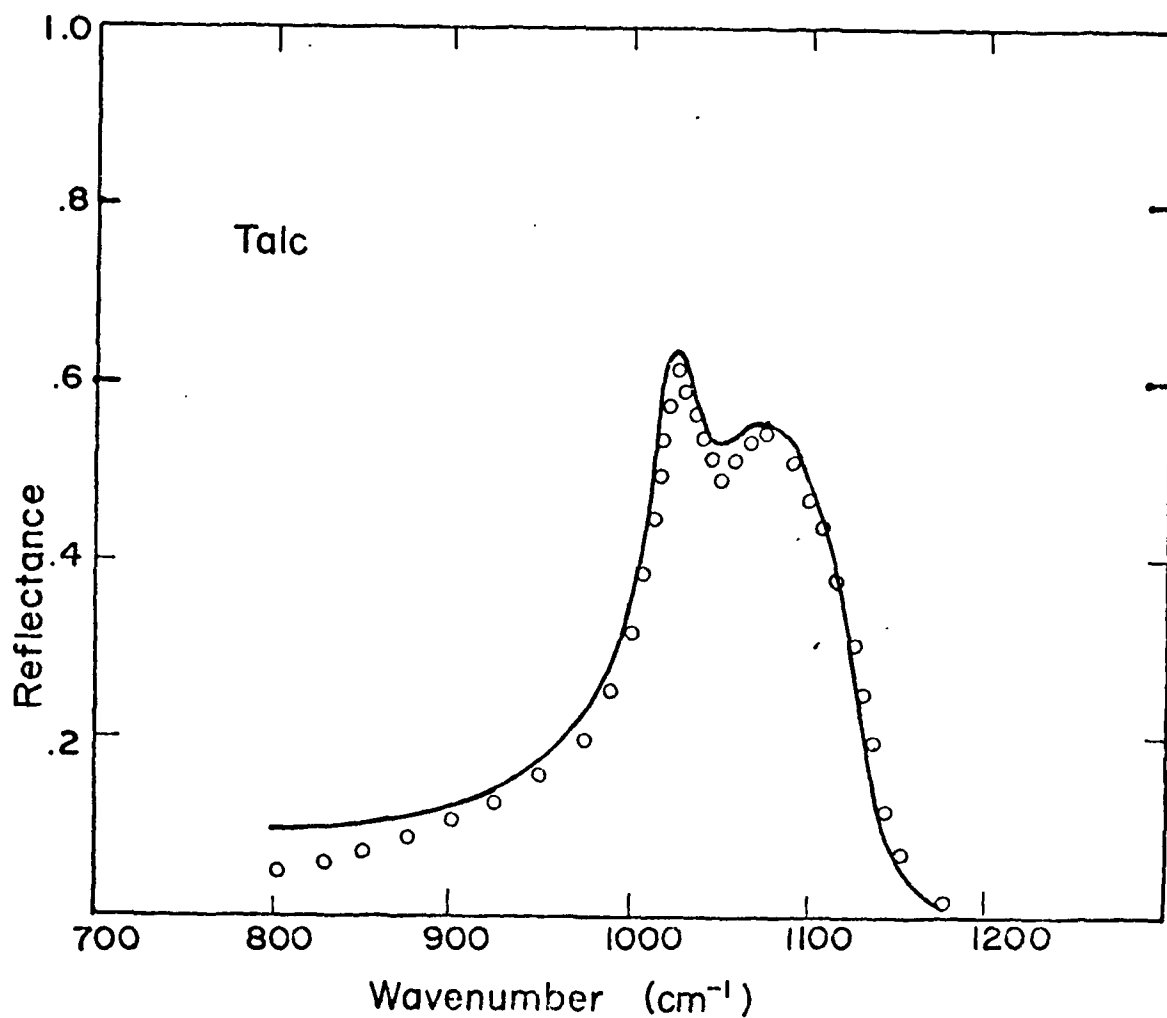


Fig. 12: Measured specular reflectance (solid line) at almost-normal incidence for a pressed powder sample of talc and an oscillator fit (circles) used to determine optical constants.

predominate shape rather than a wide distribution of shapes as called for by our CDE theory. Since talc is a layered silicate, in this sense similar to mica, the particles may be mostly platelets. With this as a working hypothesis we were able to fit the main peak of the extinction data for talc using calculations for a highly flattened, single ellipsoid (with geometrical factors of  $L_1=L_2=.01$ ,  $L_3=.98$ , for example). The results of this fit give a spectrum of optical constants in rather good agreement with the results from reflection measurements, although the flattened ellipsoid calculations give an additional absorption band near  $1130\text{ cm}^{-1}$  as plotted in fig. 11 which is not present in the measurements. Because of the difficulty with inversion of the extinction data, which we have not been able to completely resolve, we feel that in this case the reflectance technique has given us the most reliable optical constants. Both sets of oscillator parameters are given in the Appendix.

#### G. Amorphous Aluminum Oxide

The last solid we discuss is one available only as small particles or coatings on metal substrates. When very small aluminum particles are produced by evaporating aluminum in a helium atmosphere of about 5 Torr, aluminum smoke particles of 50 to 100 Å diameter are formed. These particles readily oxidize upon contact with air to a depth of about 10 Å from the surface, producing an aluminum oxide coating which is quite amorphous. We have found that in a similar smoke production process except for use of about 5 Torr of air rather than helium, very small aluminum oxide smoke particles are produced which are also highly amorphous. Since bulk aluminum oxide readily crystallizes, bulk samples of amorphous

$\text{Al}_2\text{O}_3$  are not available. Small particle samples such as the aluminum oxide smoke samples must be used if optical constants of the amorphous oxide are to be obtained. There has been a need to have such optical constants in order to be able to compare calculations and measurements for infrared absorption of oxide-coated aluminum particles in order to infer the amount of the oxide present. To this end we have applied the present technique of analysis to the extinction spectrum measured for amorphous aluminum oxide smoke, prepared as mentioned above, dispersed in KBr in our usual way.

Results for experimental volume-normalized extinction and the calculated fit are shown in figure 13. Oscillator parameters for the best fit are found in the Appendix. There is some difficulty in fitting the steep edge on the high frequency side of the extinction band. This may be due to the fact that amorphous materials do not have a small number of Lorentz oscillators as crystals do. The disorder of the amorphous material breaks down the selection rules so that an essentially infinite number of narrow oscillators must be used in fitting optical properties properly with Lorentz oscillators. Despite these difficulties, the fit probably gives almost as good values for optical constants as for the crystalline powders. Certainly these are the best optical constants for amorphous aluminum oxide we are aware of in the infrared region.

Although this sample does not have strong absorption bands near  $10\text{ }\mu\text{m}$  and hence is not a candidate for  $8 - 12\text{ }\mu\text{m}$  obscuration, the technique has provided useful optical constants for an important solid which cannot be obtained using conventional bulk solid techniques.

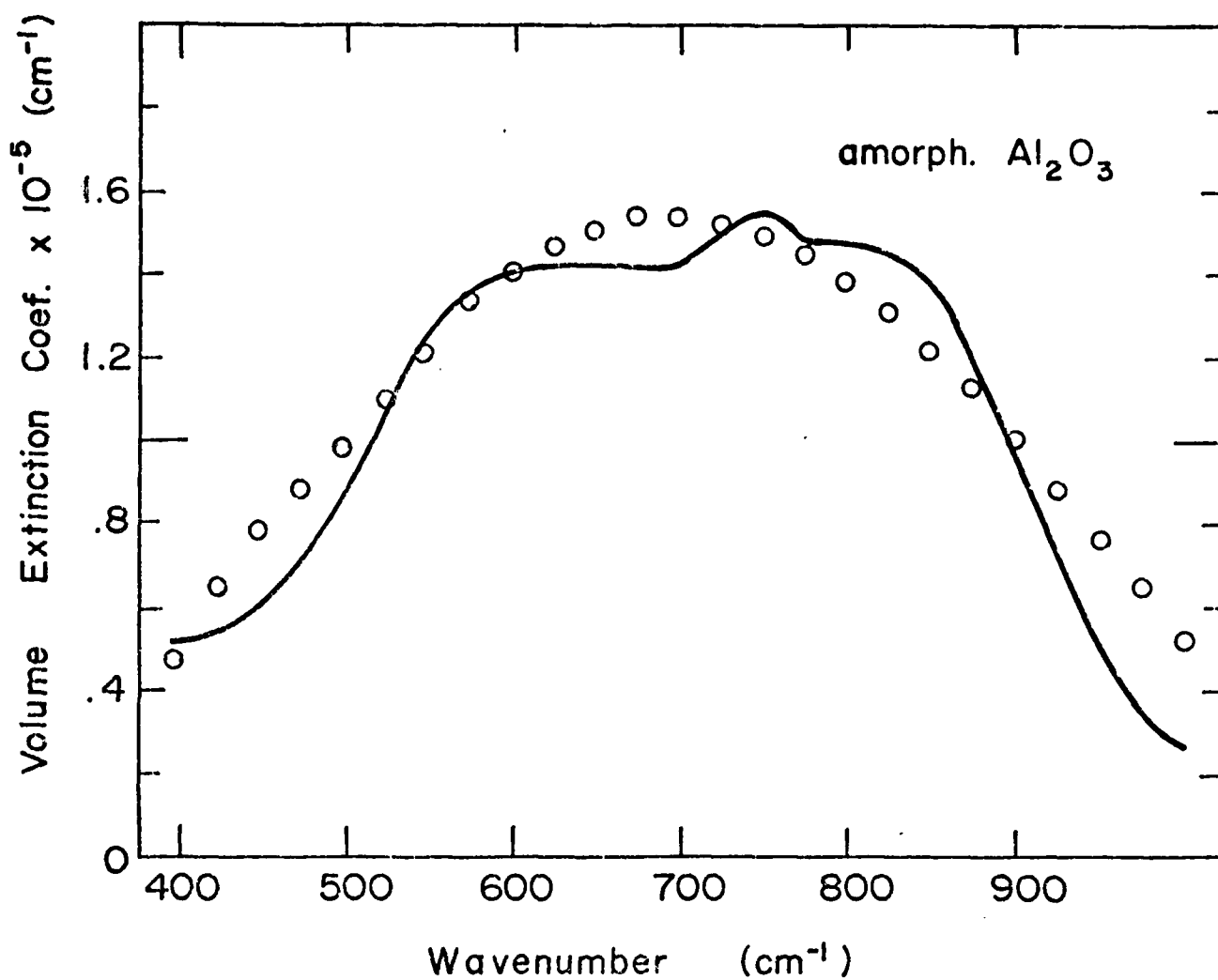


Fig. 13: Volume-normalized extinction measured for amorphous aluminum oxide smoke particles dispersed in KBr (solid curve) compared with the theoretical fit (circles) used to infer optical constants summarized in the Appendix.

## VI. CONCLUDING REMARKS

The technique described in this report for determining optical constants of powdered materials should give results that are reasonable for materials that fit the following criteria:

- (1) single component materials such as single minerals
- (2) isotropic optical constants as for cubic crystals or amorphous solids
- (3) existing in a very irregular distribution of particle shapes

By these restrictions the techniques should be best for solids like obsidian and the amorphous aluminum oxide. Even for a single component material (such as the mineral montmorillonite) when the infrared optical constants are anisotropic (different in different directions) our procedure is not strictly correct. If we knew which absorption features were due to certain directions in the solid, we could probably take this into account, as was done for the highly anisotropic solid  $\alpha$ - $\text{Al}_2\text{O}_3$  with good results in figure 1. In that case we were solving the direct problem rather than the more difficult inverse problem, however. We were working from known, bulk optical constants to calculate small particle extinction. When working backward from small particle extinction to bulk optical constants one does not know the dependence of measured absorption on crystallographic direction. Thus the optical constants we have derived must properly be considered as some sort of averaged optical constants, in this case averaged over the various directions. As is the case for any averaged quantity the results should be appropriate for application in an experiment which averages in the same way. The results cannot be guaranteed to be accurate in applications to other experiments. We would caution against relying on the optical constants for use in radiation

calculations for the earth's atmosphere where the important calculated quantity may be the single particle albedo or the back scatter - to - forward scatter ratio.

An even more difficult problem is presented when one considers a mixture of mineral components. This may be the situation for the volcanic dust. More certain difficulties would result from attempting to apply this technique to a soil sample or a collection of atmospheric dust, both of which would surely be composed of a mixture of various kinds of pure solids or minerals. One could apply the technique to get "effective optical constants", but again they would only be sure to apply to the exact experiment from which they were extracted. For these reasons we have not applied the technique for obtaining optical constants to samples such as the standard "Arizona Road Dust", a standard soil sample that has been much studied. In fact we have perhaps already pushed the technique a little too far in applying it to talc, serpentine, and Mt. St. Helens dust. A large amount of further work will doubtless have to be done before it will become obvious how useful effective optical constants of mixtures are, and under what circumstances their use is appropriate. The optical constants derived in this work are probably the best available in certain cases. Nevertheless, being thus warned the reader can use discretion in application of the results.



## REFERENCES

- Barker, A. S., 1963, Phys. Rev. 132, 1474.
- Carlson, H. R., 1980, Appl. Opt. 19, 1165.
- Chen, T. S., F. W. de Wette, and L. Kleinman, 1978,
- Day, K. L., T. R. Steyer, and D. R. Huffman, 1974,  
Astrophys. J. 191, 415.
- Dayawansa, I. J., and C. F. Bohren, 1978, Phys. Stat. Sol. (b),  
86, K27-30.
- Dorschner, J. C., C. Friedemann, and J. Gürtler, 1978,  
Astron. Nachr. 299, 269.
- Dowling, J. M., and C. M. Randall, 1977, Aerospace Final  
Report, AFRPL-TR-77-14.
- Fuchs, R., 1975 Phys. Rev. B11, 1732.
- Fuchs, R., 1978, Phys. Rev. B18, 7160.
- Genzel, L., 1975, Festkörperprobleme Vol. XIV, ed. by H. J.  
Queisser (Vieweg: Braunschweig).
- Genzel, L. and T. P. Martin, 1973, Surf. Sci. 34, 33.
- Genzel, L. and T. P. Martin, 1972, Phys. Stat. Sol. B51, 91.
- Häfele, H. G., 1963, Ann. Phys. 10, 321.
- Hunt, A. J., T. R. Steyer, and D. R. Huffman, 1973,  
Surf. Sci. 36, 454.
- Huffman, D. R., 1979, Final Report on Naval Air Systems Command  
Contract N00019-78-C-0479.
- Huffman, D. R., 1977, Adv. in Phys. 26, 129.
- Huffman, D. R., 1980, in NRL Memorandum Report 4197, ed. A.  
Deepak and L. H. Ruhnke, (Naval Research Lab: Washington).
- Huffman, D. R., and C. F. Bohren, 1980, in Light Scattering by  
Irregularly Shaped Particles, ed. D. W. Schuerman,  
Jasperse, J. R., A. Kahan, J. N. Plendl, and S. S. Mitra, 1966,  
Phys. Rev. 146, 526.

June, K. R., 1972, Appl. Opt. 11, 1655.  
Lindberg, J. D., 1975, Opt. and Quantum Elec. 7, 131.  
Mic, G., 1908, Ann. Phys. 25, 377.  
Neuroth, N., 1955, Glastech. Ber. 28, 411.  
Spitzer, W. G., and D. A. Kleinman, 1961, Phys. Rev. 121, 1324.  
Stern, F., 1963, Solid State Physics 15, ed. F. Seitz and  
D. Turnbull (Academic Press:New York).  
Steyer, T. R., K. L. Day, and D. R. Huffman, 1974, Appl. Opt.  
13, 1586.  
Zolotarev, V. M., 1970, Opt. Spectrosc. 29, 34.

# APPENDIX

## Oscillator Parameters for Calculating Optical Constants of Materials Studied in This Work

Material (freq. range - $\text{cm}^{-1}$ )	$\epsilon_0$	$\omega_j$	$\gamma_j$	$\omega_{pj}$	Fig. No.
A. Obsidian (900-1300)	2.40	1035 1160 990 438	70 165 50 48	750 325 430 560	5,6
B. Serpentine (800-1200)	2.70	935 1070 1015	35 50 120	675 270 300	7
C. Chlorite (800-1150)	2.62	940	100	800	8,9
D. Montmorillonite (800-1300)	2.25	1015 1140 890	70 120 60	610 250 200	10
E. Mt. St. Helens Dust (850-1300)	2.25	995 1070 1150	90 80 120	810 330 280	10
F. Talc - Refl. Fit (800-1200)	2.25	1017 1045	15 52	605 385	12
Talc - Ellipsoid Fit (900-1200)	2.25	1015	17	250	11
G. Amorphous $\text{Al}_2\text{O}_3$ (400-1000)	2.30	420 530 470	150 160 180	1328 838 1559	13

END

DATE  
FILMED

6-8-11

DTIC